Functionalized monolayers on mesoporous silica and on titania nanoparticles for mercuric sensing†

Eunjeong Kim, Sungmin Seo, Moo Lyong Seo and Jong Hwa Jung*

Received 4th August 2009, Accepted 4th November 2009
First published as an Advance Article on the web 13th November 2009
DOI: 10.1039/b915975d

Heterogeneous "naked-eye" colorimetric and spectrophotometric cation sensors were prepared by immobilization of an azobenzene-coupled receptor onto mesoporous silica (**AR-SiO_2**) or titania nanoparticles (**AR-TiO_2**) *via* sol–gel or hydrolysis reactions. The optical sensing ability of **AR-SiO_2** was studied by addition of metal ions such as K^+, Ca^{2+}, Sr^{2+}, Co^{2+}, Cd^{2+}, Pb^{2+}, Zn^{2+}, Fe^{3+}, Cu^{2+} and Hg^{2+} ions (all as chlorides) in aqueous solution. Upon the addition of Hg^{2+} ion in suspension, the **AR-SiO_2** resulted in a color change from yellow to deep red. No significant color changes were observed in the parallel experiments with K^+, Ca^{2+}, Sr^{2+}, Co^{2+}, Cd^{2+}, Pb^{2+}, Zn^{2+}, Fe^{3+} or Cu^{2+} ion. These findings confirm that the **AR-SiO_2** can be useful as chemosensors for selective detection of Hg^{2+} ion over a range of metal ions in aqueous solution. Also, the color change of **AR-SiO_2** was independent of the presence of anions NO_3^-, ClO_4^-, Br^- and I^-. We also prepared a portable chemosensor kit by coating a 4 μm thick film of **AR-TiO_2** onto a glass substrate. We found that this **AR-TiO_2** film detects Hg^{2+} ion at pH 7.4 with a sensitivity of 28 nM. Finally, we tested the effect of pH on **AR-TiO_2** with Hg^{2+} ion between pH 1.0 to 11.0. The absorbance and color changes of **AR-TiO_2** were almost constant between pH 4 and 11. The results imply that the **AR-TiO_2** film is applicable as a portable colorimetric sensor for the detection of Hg^{2+} ion in the environmental field.

Introduction

Chemical sensors are molecular receptors that transform into analytically useful signals upon binding to specific guests. Such sensors have attracted interest in fields such as waste management, environmental chemistry, clinical toxicology, and bioremediation of radionuclides due to their potential for easy detection, and quantification of pollutant species.[1–9] Among these, the selective detection of metal ions such as mercury and lead is critical for environmental monitoring, as these are highly toxic and common pollutants.

Various approaches for mercury screening, including atomic absorption/emission spectroscopy and inductively coupled plasma mass spectrometry, have been investigated.[10–12] Although these instrumental analyses are currently used in applications relevant to the detection of metal toxins, there is still a need to develop inexpensive and simple methods for the detection of metal toxins. Among the various sensor approaches, optical sensors that allow on-site, real-time, qualitative, or semi-quantitative detection without the use of bulky or complex spectroscopic instrumentation have received a great deal of attention as promising methods for the determination of pollutant species in environmental analysis.[13–16] However, most of the sensors developed so far are kinetically slow with a limited sensitivity for detection below the permissible level of metal toxins, indicating a lack of control of the remote sensing of pollutant species.

Very recently, organic-inorganic hybrid materials have been investigated as new materials for ion recognition and sensing. Receptors immobilized on inorganic nanomaterials such as SiO_2, Al_2O_3 and TiO_2 constitute solid chemosensors and, as such, have important advantages when used in the heterogeneous solid-liquid phase.[17–28] Firstly, receptors immobilized on an inorganic support can remove the guest molecules (toxic metal ions or anions) from the pollutant solution. Secondly, the inorganic oxides can be fabricated as functionalized porous nanomaterials. In particular, nanocrystalline TiO_2 films are potentially useful materials for optical sensors due to their high surface area and excellent optical transparency in the visible region of the spectrum ($\lambda > 400$ nm).

Mesoporous silica and titania nanoparticles (SBA-15 and MCM-41) are promising as inorganic support materials due to their homogeneous porosity and large surface area. Only limited examples of such heterogeneous sensors have been reported,[17–28] however. Such sensors take advantage of the independent solubility of the receptor in water and in organic solvents. Very recently, for example, Martínez-Máñez *et al.* reported on a fabrication of the squaraine-based receptor immobilized on a mesoporous 3D hybrid material for Hg^{2+} ion detection and adsorption.[29] Addition of the colorless hybrid material to a solution containing Hg^{2+} ion resulted in a rapid and dramatic change to deep blue. The solution also showed a remarkable fluorescence. However, the hybrid material could not be renewed after adsorption of Hg^{2+} ion because it acts as the chemodosimeter for these ions. In addition, this hybrid material was selectively detectable for Hg^{2+} in a mixed solvent of acetonitrile

Department of Chemistry, Research Institute of Natural Science, Environmental Biotechnology National Core Research Center, Gyeongsang National University, Jinju, 660-701, Korea. E-mail: jonghwa@gnu.ac.kr

† Electronic supplementary information (ESI) available: Measurement data. See DOI: 10.1039/b915975d

and water due to the solubility of the squaraine receptor at high Hg^{2+} concentration.

Furthermore, Willner *et al.* reported that oligonucleotides immobilized on gold nanoparticles enabled the colorimetric detection of Hg^{2+}.[30] The gold nanoparticles were highly aggregated in the presence of Hg^{2+} ion, which changed from red to blue. Also, the gold nanoparticles were not renewable after adsorption of Hg^{2+} ion.

Based on this idea, in this work we explore a new approach to the development of nanomaterial chemosensors. We synthesized the azobenzene-coupled acyclic receptor **6** containing a triethoxylsilane moiety (Scheme 1) and immobilized **6** onto the surface of mesoporous silica by sol–gel reaction. We also attached **4** containing a carboxylic acid to titania nanoparticles of 50 nm diameter in order to prepare a portable chromogenic sensor. The receptors **4** and **6** were immobilized by different methods on the two different supports. To the surface of mesoporous silica, the receptors were attached by covalent bonds *via* a sol–gel grafting method. To the TiO_2 nanoparticles, the receptors were attached *via* hydrogen bonds. After immobilizing the receptors, we transformed the ester of receptor **4** or **6** into an acid-type receptor attached onto mesoporous silica and titania by hydrolysis. We herein describe the fabrication of an acyclic acid-type receptor immobilized on mesoporous silica (**AR-SiO_2**) and the same receptor on titanium oxide nanoparticles (**AR-TiO_2**), both of which selectively change color upon the addition of Hg^{2+}.

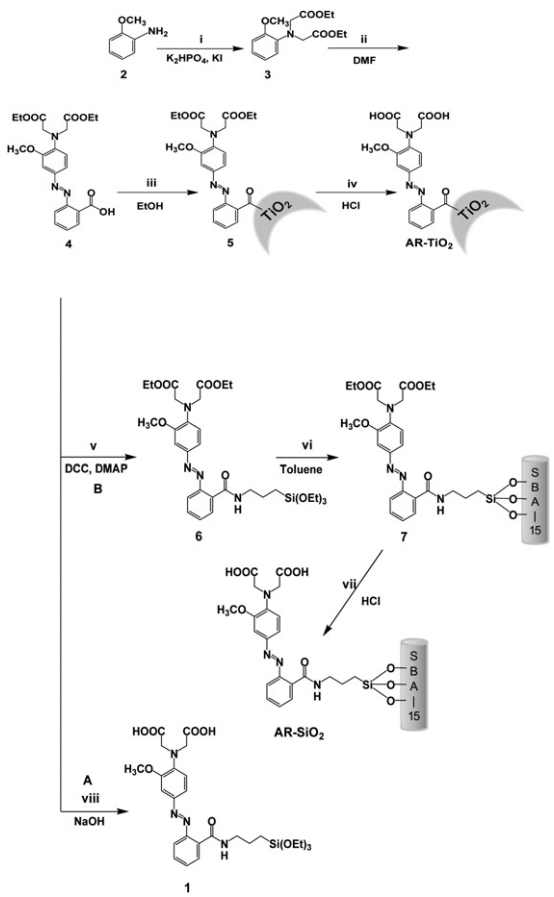

Scheme 1 Synthetic method. Reaction conditions: (i) $BrCH_2CO_2Et$, 60 °C; (ii) diazonium salt, DMF, 0 °C; (iii) TiO_2 nanoparticles, reflux; DMF = *N*,*N*′-dimethylformamide; (iv) HCl, methanol; (v) 3-Aminopropyltriethoxysilane, DCC, DMAP, EA, RT; (vi) mesoporous silica, toluene, reflux; (vii) HCl, methanol; (viii) NaOH.

Experimental

Characterization

^1H and ^{13}C NMR spectra were recorded on a Bruker 300 apparatus. Infrared spectra of silica powder pellets were obtained using a Shimadzu FT-IR 8400S and the mass spectrum was obtained with a JEOL JMS-700 mass spectrometer. Powder X-ray diffraction patterns were recorded on a Siemens D8 Advance diffractometer using Cu-Kα radiation and a secondary monochromator. Transmission electron microscopy (TEM) images were captured with a JEOL JEM – 2100 F microscope. Nitrogen-adsorption isotherms were measured at 78 K on a Micromeritics ASAP 2010 analyzer. Thermal gravimetry analysis was conducted on a TA SDT Q600 with a heating rate of 10 °C min^{-1} using a Pt pan in air. The temperature was scanned from 25 °C to 900 °C.

Preparation of mesoporous silica

Mesoporous silica was synthesized starting from the preparation of a hydrochloric acid solution of P-123 [(poly(ethylene oxide)-poly(propylene oxide)-poly(ethylene oxide) triblock copolymer)]. Tetraethyl orthosilicate (TEOS) was then added and the mixture was stirred at 40 °C for 20 h. The molar composition was 1 : 5.9 : 193 : 0.017 TEOS : HCl : H_2O : P-123. The solid was aged at 65 °C for 1 day and then was filtered, washed and dried at 90 °C. To cleave the template to generate mesopores, 1.0 g of as-synthesized SBA-15 was mixed with 100 mL of 60 wt % H_2SO_4 solution and refluxed at 95 °C for 1 day. The product was recovered by washing with water and dried at 90 °C. To generate mesopores, the acid-treated sample was heated to 200 °C in air. To remove cationic surfactants from the resulting dried fiber-like flocculates and particles, the sample was calcined in a box furnace in air at 500 °C for 5 h, with a ramp rate of 1 °C min^{-1}.

Immobilization of receptor 6 onto mesoporous silica

Compound **6** (100 mg) was dissolved in toluene (10 mL). The mesoporous silica (100 mg) was added as a solid. The suspension of silica was stirred in under reflux conditions for 24 h in toluene. Then, the collected solid was washed copiously with toluene (50 mL) to rinse away any surplus **5** and dried under vacuum.

Hydrolysis of mesoporous silica immobilized with 6

To obtain the acid from the receptor (**7**) attached to mesoporous silica, the mesoporous silica immobilized with receptor **6** was first dispersed in methanol (2 mL). The suspension of silica was maintained for 10 h at room temperature. After filtration, the solid product was washed with Na_2CO_3 solution and water and dried.

Preparation of TiO_2 nanoparticles

The TiO_2 nanoparticles were obtained by a method reported previously.[25]

Preparation of receptor 4 immobilized TiO_2 films

TiO_2 paste was prepared from a sol–gel colloidal suspension containing 12.5 wt% TiO_2 and 6.2 wt% Carbowax 20000. The nanocrystalline TiO_2 particles were synthesized by the following procedure: 20 mL of titanium iso-propoxide (Aldrich Co.) were injected into 5.5 g of glacial acetic acid under argon atmosphere and stirred for 10 min. The mixture was transferred into a flask containing 120 mL of 0.1 M nitric acid at room temperature and stirred vigorously. The flask was left uncovered and heated at 80 °C for 8 h. After cooling, the solution was filtered using a 0.45 mm syringe filter, diluted to 5 wt% TiO_2 by adding H_2O and then autoclaved at 220 °C for 12 h. The colloids were re-dispersed with a 60 s cycle burst from an LDU Soniprobe. Finally, the solution was concentrated to 12.5 wt% TiO_2 on a rotary evaporator using a membrane vacuum pump at a temperature of 40 °C. Carbowax 20.000 was added and the resulting paste was stirred slowly overnight to ensure homogeneity. For the film TiO_2 preparation, 3 mL of the solution detailed above were spread on glass slides with a glass rod and using adhesive tape as spacers. After the films were dried in air, they were sintered at 450 °C for 20 min. All samples used in this work were films of 4 μm thickness. Functionalization of the TiO_2 films was achieved by immersing the films in a 1 mM solution of receptor **4** in 1 : 1 acetonitrile/*tert*-butyl alcohol mixture overnight, followed by rinsing in ethanol to remove unadsorbed receptor **4**.

Coloration and extraction of metal ions by AR-SiO_2 particles and AR-TiO_2 films

The **AR-SiO_2** (10 mg) was added to metal ion solutions (5.0 equiv with respect to **1** anchored to the **AR-SiO_2**). The mixture was stirred for 10 min. After filtration, the concentration of metal ions was analyzed by ICP (DX-500, DIONEX). The UV-vis spectra of metal-loaded **AR-SiO_2** were measured by a Shimadzu UV-2401 PC UV-Vis spectrophotometer. In addition, the reversibility of metal adsorption was measured. EDTA (10.0 μM, 2 mL) was added to the **AR-SiO_2** suspension (at pH 7.4) to remove Hg^{2+} ion bound to **AR-SiO_2**. Then, the UV-vis absorption change of the H_2O suspension of **AR-SiO_2** was measured. In addition, the **AR-TiO_2** films were dipped in cation aqueous solutions of interest in buffered condition, and then dried in air, with changes in coloration noted by visual inspection as well as by measurement of UV-vis absorption.

Compound 3

To a 50 mL round bottom flask, *o*-anisidine (**2**) was added to ethylbromoacetate in potassium dihydrogen phosphate in CH_3CN (10 mL). The reaction mixture was maintained for 10 h at 60 °C. After cooling to room temperature, the reaction mixture was reduced, then was dissolved into $CHCl_3$ (50 mL) and washed with water (2 × 30 mL). The organic phase was dried over $MgSO_4$ and reduced to oil. The crude product was purified on a silica column using 70 : 30 Hex : EtOAc to produce **3** as a white solid. Properties of **3** are as follows: m.p. 78–80 °C; ^{1}H NMR (300 MHz, $CDCl_3$, TMS) $\delta = 6.87$ (d, ^2J(H,H) = 12.3 Hz, 1H; Ar–H), 4.20 (d, ^2J (H,H) = 7.2 Hz, 1H; Ar–H), 3.80 (s, 3H; CH_3) 1.26 (t, ^3J(H,H) = 7.2 Hz, 6H; CH_3); ^{13}C NMR (300 MHz, $CDCl_3$, TMS) $\delta = 171$, 151, 122, 120, 119, 111, 77, 77, 77, 76, 60, 55, 53, 30, 14; IR (KBr): $\nu = 3393$, 3090, 2931, 2853, 1740, 1653, 1373, 1032, 751 cm^{-1}; High resolution mass spectrum (HRMS) (FAB$^+$) *m*/*z* 295.14 [(M + H)$^+$ calcd for $C_{15}H_{21}NO_5$:295.16]. Anal. Cald for $C_{15}H_{22}NO_5$: C, 61.00; H, 7.17; N, 4.74. found: C, 60.68; H, 7.23; N, 4.69.

Compound 4

To a 50 mL round bottom flask, *o*-amino benzoic acid (1.047 g, 7.5 mmol) was added which contained a solution of 1 : 1, THF : H_2O (20 mL) and $NaNO_2$ (0.5261 g, 7.6 mmol). While this mixture was being stirred at 0 °C, HCl (1.0 mL, 12 M) was slowly added. The resulting solution was added dropwise to a 100 mL single neck round bottom flask containing the appropriate ester (**3**) (6.8 mmol) in a solution of 1 : 1 THF : H_2O (40 mL). This solution was held at 0 °C for approximately 2 h and then was left stirring overnight at room temperature. The resulting dark red solution was reduced down, dissolved into $CHCl_3$ (60 mL) and washed with water (2 × 30 mL). The organic phase was dried over $MgSO_4$ and reduced to oil. The crude product was purified on a silica column using 70 : 30 Hex : EtOAc, to produce **4** as a bright red solid. Properties of **4** are as follows: m.p. 101–103 °C; ^{1}H NMR (300 MHz, $CDCl_3$, TMS) $\delta = 8.10$ (d, ^2J(H,H) = 7.75 Hz, 1H; Ar–H), 7.59 (d, ^2J(H,H) = 7.2 Hz, 1H; Ar–H), 7.48 (t, ^3J(H,H) = 7.8 Hz, 1H; Ar–H), 6.9 (d, ^2J(H,H) = 4.5 Hz, 1H; Ar–H), 4.18 (m, 8H), 3.8 (s, 3H; CH_3), 1.26 (t, ^3J(H,H) = 7.2 Hz, 6H; CH_3); ^{13}C NMR (300 MHz, $CDCl_3$, TMS) $\delta = 187$, 182, 154, 144, 135, 134, 134, 133, 133, 127, 127, 125, 120, 116, 58, 43, 42, 23, 18,; IR (KBr): $\nu = 3414$, 3270, 2940, 2856, 1870, 1735, 1637, 968, 804 cm^{-1}; HRMS (FAB$^+$) *m*/*z* 443.17 [(M + H)$^+$ calcd for $C_{22}H_{25}N_3O_7$: 443.20]. Anal. Cald for $C_{22}H_{25}N_3O_7$: C, 59.59; H, 5.68; N, 9.48. found: C, 60.11; H, 5.80; N, 9.35.

Compound 6

To a 20 mL round bottom flask, **4** (250 mg, 0.42 mmol) was added to aminopropyltriethoxysilane (1.0 g, 5.58 mmol) in ethyl acetate (10 mL). The mixture was stirred under nitrogen for two minutes and then cooled to 0 °C. 1-Hydroxybenzotriazole (HOBt, 68 mg, 0.5 mmol) and dicyclohexyl carbodiimide (DCC, 1.870 g, 9.07 mmol) were added simultaneously as a mixture of solids. The reaction mixture was allowed to warm to room temperature and stirred for 24 h. The precipitate was removed by filtration. The filtrate was then washed with aq. $NaHCO_3$ (satd.) and aq. $NaHSO_4$ (satd.). The solution was dried with $MgSO_4$ and the solvent was removed by rotary evaporation to produce a reddish crude. This crude product was purified by column chromatography (silica-gel, n-hexane: ethyl acetate, 1 : 1, R_f 0.45) to give the product (1.24 g, 65%). Properties of **6** are as follows: m.p. 115–117 °C; ^{1}H NMR (300 MHz, DMSO) $\delta = 7.5$, 7.5, 7.4 (m, 3H) 6.9, 6.8, 6.8, 6.7 (m, 4H), 4.17 (t, ^3J(H,H) = 6.9 Hz, 1H; Ar–H), 3.79 (s, 3H), 1.73 (t, ^3J(H,H) = 2.4 Hz, 1H; Ar–H) 1.24 (m, 15H); IR (KBr): $\nu = 3414$, 3270, 2940, 2856, 1870, 1735, 1637, 1121, 968, 804 cm^{-1}; HRMS (FAB$^+$) *m*/*z* 646.30 [(M + H)$^+$ calcd for $C_{31}H_{46}N_4O_9Si$: 646.34]. Anal. Cald for $C_{31}H_{46}N_4O_9Si$: C, 57.56; H, 7.17; N, 8.66. found: C, 57.71; H, 7.02; N, 8.33.

Compounds 5 and 7

The synthetic methods will be described in detail later.

Results and discussion

Synthesis of acyclic azobenzene-based receptor

The synthesis of the target compound **1** is difficult due to the polymerization of the triethoxyl group during hydrolysis, which removes the ethyl groups of **4** by pathway A in Scheme 1. Thus, we tried to obtain **1** by hydrolysis of **4** in acidic conditions after immobilization of receptor **6** onto the surface of mesoporous silica by pathway B. To prepare a selective chromogenic receptor for Hg^{2+}, we began with **2**, then formed *o*-anisidine (**3**) by alkylation using two equivalents of ethylbromoacetate in the presence of potassium dihydrogen phosphate and potassium iodide in CH_3CN. The azobenzene ester **4** was made by the reaction of the diazonium salt of *o*-aminobenzoic acid with **3**. Subsequently, treatment with **4** and aminopropyltriethoxysilane as precursor for the sol–gel reaction afforded compound **6** as a yellow powder. Then, immobilization of the chromogenic receptor **6** to mesoporous silica was conducted under reflux for 24 h in toluene. In this process, the triethoxylsilyl group of **6** attached onto mesoporous silica undergoes hydrolysis and attaches covalently to the surface of the mesoporous silica.[15] After cooling to room temperature, the yellow solid product was filtered, washed with THF, and dried. Finally, a chemosensing material was obtained as a light yellow solid by hydrolysis of **7** attached onto mesoporous silica under acidic conditions. The acyclic receptor **1** immobilized mesoporous silica (**AR-SiO$_2$**) was characterized by transmission electron microscopy (TEM), UV-vis spectroscopy, thermogravimetric analysis (TGA) and FT-IR.

Preparation of AR-SiO$_2$

In Fig. 1 and Fig. S1 (ESI),† TEM images of **AR-SiO$_2$** and the mesoporous silica clearly show the formation of a well-ordered hexagonal arrangement of mesoporous channels before and after attaching the receptor **1**. To investigate the porosity changes of the mesoporous silica induced by the introduction of the azobenzene-coupled derivative **1**, we measured the surface area, pore volumes and pore diameters of both mesoporous silica and **AR-SiO$_2$** using nitrogen adsorption-desorption isotherms (Fig. 1B). The mesoporous silica has a BET (Brunauer-Emmett-Teller) surface area of 1119.72 $m^2\ g^{-1}$ and a pore volume of 0.49 $cm^3\ g^{-1}$. On the other hand, we observed that the **AR-SiO$_2$** has a BET surface area of 673.21 $m^2\ g^{-1}$ and a pore volume of 0.26 $cm^3\ g^{-1}$. The mesoporous silica and the **AR-SiO$_2$** have BJH (Barrett-Joyner-Halenda) pore diameters of 2.24 and 2.15 nm, respectively (Fig. S2, ESI).† The decreased surface area and pore diameter in **AR-SiO$_2$** are attributable to the attachment of the acyclic azo-coupled derivative to the mesoporous silica. Furthermore, from the results of the TGA measurement (Fig. S3, ESI),† we determined that the **AR-SiO$_2$** consists of only 18.0 wt% of **1**.

For further structural proof of the **AR-SiO$_2$**, we carried out IR spectroscopy of both mesoporous silica and **AR-SiO$_2$**. For the mesoporous silica, IR peaks appear at 3450, 1658 and 1084 cm^{-1}. For **AR-SiO$_2$** (Fig. S4, ESI),† peaks appear at 3382, 2976, 2933, 2884, 1626, 1615, 1570, 1471, 1446, 1428 and 1382 cm^{-1}. These new peaks originate from the acyclic azo-coupled receptor **1**, providing solid evidence that **1** is indeed attached to the surface of the mesoporous silica.

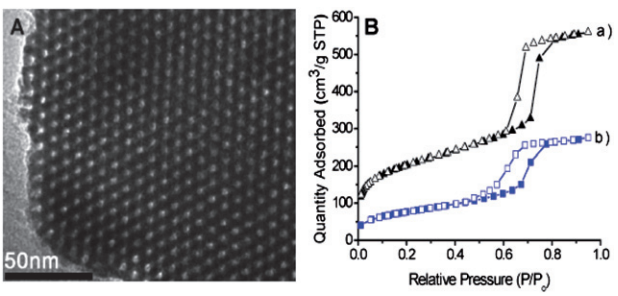

Fig. 1 (A) TEM image of **AR-SiO$_2$**. (B) The nitrogen adsorption-desorption isotherms of (a) mesoporous silica and (b) **AR-SiO$_2$**.

Preparation of the azobenzene-based receptor 4 immobilized TiO_2 film (AR-TiO_2)

In consideration of extending its usefulness, immobilization of the chromogenic receptor **4** into the TiO_2 nanoparticles was conducted under reflux conditions for 24 h in toluene. In this process, the receptor **4** undergoes hydrolysis and attaches covalently to the surface of TiO_2.[9,13] After cooling to room temperature, the red solid product was filtered, washed with ethanol, and then dried. For the structural proof of the TiO_2, we took IR spectroscopy of both TiO_2 and **AR-TiO$_2$**. For TiO_2, IR peaks appear at 3391, 1639 and 655 cm^{-1} whereas for **AR-TiO$_2$** appeared at 3421, 2977, 2926, 2874, 1728, 1633, 1594, 1513, 1439, 1371, 1284, 1131, 1069 and 655 cm^{-1} (Fig. S5, ESI)† where new peaks are originated from azobenzene-coupled receptor **4**, giving us a solid evidence that **4** is certainly attached onto the surface of the TiO_2 nanoparticles. In addition, TEM images of TiO_2 nanoparticles and **AR-TiO$_2$** were observed (Fig. 2). Both TiO_2 nanoparticles before and after immobilization of the receptor **4** showed 30∼60 nm of diameters without any morphological change.

To prepare **AR-TiO$_2$** films onto glass slides, 3 mL of the solution detailed above were spread on the glass slides with a glass rod and using adhesive tape as spacers. After the films were dried in air, they were sintered at 450 °C for 20 min. Sensitization of the TiO_2 films was achieved by immersing the films in a 1.0 mM solution of receptor **4** in 1 : 1 acetonitrile/*tert*-butyl alcohol overnight, followed by rinsing in ethanol to remove

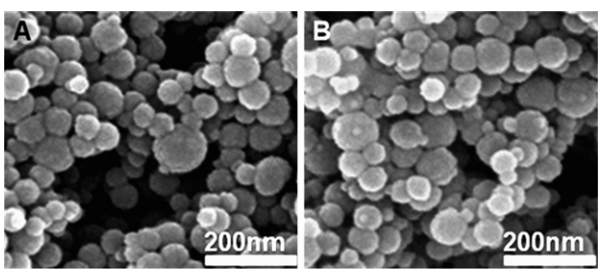

Fig. 2 TEM image of (A) TiO_2 and (B) **AR-TiO$_2$** nanoparticles.

unadsorbed receptor **4**. Finally, the slight yellow color of the **AR-TiO$_2$** film was obtained.

Coloration of AR-SiO$_2$ with metal ions

We investigated the spectroscopic properties of the **AR-SiO$_2$** towards the metal ions K^+, Ca^{2+}, Sr^{2+}, Co^{2+}, Cd^{2+}, Pb^{2+}, Zn^{2+}, Fe^{3+}, Cu^{2+} and Hg^{2+} in aqueous solution (pH = 7.4, 5.0 equiv with respect to **1** anchored to the mesoporous silica). Interestingly, upon the addition of Hg^{2+} in H_2O suspension, **AR-SiO$_2$** resulted in a color change from light yellow to red within 10 s (Fig. 3A(b) and 3B(b)). In this category of chromophore, photoexitation causes a net electronic charge transfer from the donor end (bridgehead nitrogen) to the acceptor end within the chromophore. Thus, the observed color change is ascribed to the formation of a complex with strong coordination bonding between the bridgehead nitrogen atom of aniline group of **1** and Hg^{2+}.[7,23] Except for Hg^{2+}, no significant color changes were observed in the experiments using other metal ions (Fig. 3A(c–i) and Fig. S6, ESI).† These findings confirm that **AR-SiO$_2$** can be useful as a colorimetric sensing material for the selective detection of Hg^{2+} in the presence of other metal ions. This is a rare example of chromogenic sensing for a specific metal ion by functional inorganic nanomaterials. The association constant (K) for the Hg^{2+} coordination to **AR-SiO$_2$** was calculated to be 3.05×10^5 M^{-1} (log $K = 5.48$).[28]

The UV-vis spectrum of Hg^{2+}-loaded **AR-SiO$_2$** is unchanged in the presence of an excess amount of K^+, Ca^{2+}, Sr^{2+}, Co^{2+}, Cd^{2+}, Pb^{2+}, Fe^{3+}, Cu^{2+} and Zn^{2+} (Fig. S7, ESI),† indicating that **AR-SiO$_2$** shows great promise as a selective chemosensor for the detection of Hg^{2+}.

To develop the **AR-SiO$_2$** as a general mercury cation sensor which is independent of the anion present, we investigated the anion effect by addition of other anion such as NO_3^-, ClO_4^- and Br^- (Fig. S8, ESI).† As observed for the $HgCl_2$ solution, the color of the **AR-SiO$_2$** also changed from yellow to red. This finding indicates that the **AR-SiO$_2$** can be employed for the detection of Hg^{2+} independently of the other anion(s) present.

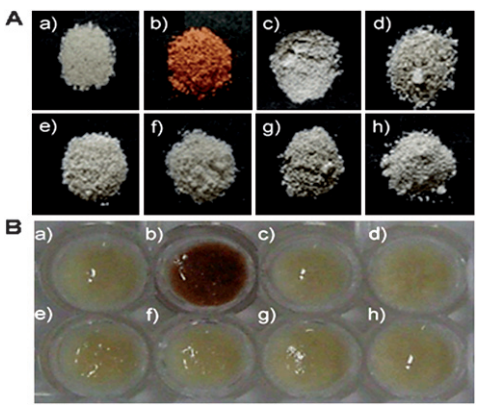

Fig. 3 The colorimetric response of (A) dried and (B) H_2O suspension samples of **AR-SiO$_2$** (5.0 mg) in the (a) absence and the presence of (b) $HgCl_2$ (5.0 equiv), (c) $CoCl_2$ (5.0 equiv), (d) $CdCl_2$ (5.0 equiv), (e) $PbCl_2$ (5.0 equiv), (f) $ZnCl_2$ (5.0 equiv), (g) $FeCl_3$ (5.0 equiv) and (h) $CuCl_2$ (5.0 equiv) at pH = 7.4.

The Hg^{2+}-loaded **AR-SiO$_2$** was isolated to confirm the binding efficiency of Hg^{2+} by **AR-SiO$_2$**. Then, the solid UV-vis spectrum for the Hg^{2+}-loaded **AR-SiO$_2$** was compared with that for **AR-SiO$_2$** alone (Fig. 4A). The Hg^{2+}-loaded **AR-SiO$_2$** spectrum exhibits an absorption maximum at 495 nm, whereas the absorption peak appears at 310 nm for the Hg^{2+}-free one, indicating that the Hg^{2+} is efficiently bound to **1** attached in the **AR-SiO$_2$** by covalent bonds.

In addition, we confirmed the reversibility of the color change of **AR-SiO$_2$** by removing the Hg^{2+} ion bound to **AR-SiO$_2$** by treatment with EDTA. As expected, the red color of **AR-SiO$_2$** in the presence of Hg^{2+} ion was changed into light yellow upon the EDTA (10.0 μM) treatment (Fig. 4B). Once again, the color change was fully reversible with the addition of EDTA (10.0 μM). Because the Hg^{2+} ion bound to **AR-SiO$_2$** is dissociated by EDTA, the **AR-SiO$_2$** can be repeatedly used by renewing with EDTA (Fig. 4C). Clearly, **AR-SiO$_2$** exhibits excellent reusability, as almost no loss in **AR-SiO$_2$** sensitivity was observed after eight repeated dipping/rinsing cycles.

In order to understand the coordination behavior between the receptor **1** attached to **AR-SiO$_2$** and the Hg^{2+} ion, we made repeated attempts to obtain the crystal structure of the complex **1** with the Hg^{2+} ion, but were not successful. As an alternative, we measured the UV-vis spectra of **AR-SiO$_2$** with the addition of Hg^{2+} ion to confirm the stoichiometry between **1** attached onto **AR-SiO$_2$** and the Hg^{2+} ion. A spectral variation of **AR-SiO$_2$** in H_2O was observed upon the gradual addition of $HgCl_2$. As a function of the Hg^{2+} concentration, a new absorption band centered at 495 nm leading to an obvious color change from light yellow to red was observed. The red-shift from 310 to 495 nm of the absorption of **AR-SiO$_2$** is attributed to a strong binding affinity between the nitrogen atom of **1** attached to **AR-SiO$_2$** and the Hg^{2+} ion (Fig. S9, ESI†).[7] The stoichiometry for the **1** complex with Hg^{2+} was examined by a Job plot. As shown in Fig. S8,† it was found that the **1**-Hg^{2+} complex concentration approaches a maximum when the molar faction of [**1**]/([**1**] + [Hg^{2+}]

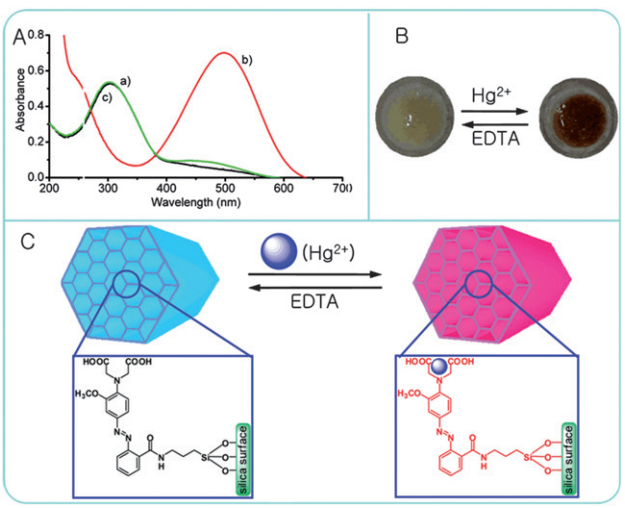

Fig. 4 (A) Solid UV-vis spectra of **AR-SiO$_2$** (5.0 mg) in the (a) absence and (b) the presence of $HgCl_2$ (5.0 equiv) and (c) after addition of EDTA (10.0 μM, 2 mL). (B) Picture and (C) proposed structure of **AR-SiO$_2$**·Hg^{2+} before and after treatment of EDTA (10.0 μM).

is about 0.5, indicating that it forms a 1 : 1 complex of **1** attached to **AR-SiO$_2$** with Hg^{2+} ion, as show in Fig. S10, ESI.†

Fig. S11 (ESI)† shows the standard calibration data (Abs. *vs.* [Hg^{2+}]) for **AR-SiO$_2$**. A linear response is observed (between 1.0 μM and 10 μM) with a sensitivity of ~1.0 μM. This sensitivity is equivalent to those previously reported for spectrophotometric sensors anchored to mesoporous aluminosilicates.[24]

The above results encouraged us to test the separation of Hg^{2+} from the waste solution. The test sample was prepared by adding **AR-SiO$_2$** (10 mg) to 1 mL of waste containing 2.0 μM Hg^{2+}. The Hg^{2+}-loaded **AR-SiO$_2$** was then removed by filtration from the waste. To determine the amount of Hg^{2+} separated by the **AR-SiO$_2$**, the amount of Hg^{2+} left in the waste solution was determined by inductively coupled plasma mass spectrometry (ICP-MS). The ICP-MS measurements indicated that only 7% of the original Hg^{2+} remained in the waste solution, suggesting that the **AR-SiO$_2$** removed 93% of the Hg^{2+}. We also analyzed the Hg^{2+}-loaded **AR-SiO$_2$** sample by UV-vis spectroscopy (Fig. S12, ESI).† The absorbance of the Hg^{2+}-loaded **AR-SiO$_2$** was 0.26, coinciding with the calibration curve (Fig. S11, ESI).†

Furthermore, we examined the pH effect on the Hg(II) uptake by measuring the absorbance of **AR-SiO$_2$** treated with Hg(II) solutions (pH 1.0–12.0). As shown in Fig. S13 (ESI),† no significant absorbance or color changes were observed between pH 2–9, suggesting the proposed **AR-SiO$_2$** sensor can be used in pH 2–9.

The extraction ability of the **AR-SiO$_2$** was also estimated by measuring the amount of Hg^{2+} ion adsorbed on the **AR-SiO$_2$** by ICP, resulting in 90% of Hg^{2+} ion being extracted by **AR-SiO$_2$**. This result suggests that the **AR-SiO$_2$** is potentially useful as a stationary phase for the separation of Hg^{2+} ion in liquid chromatography. Also, the adsorption capacity of the **AR-SiO$_2$** was measured through the solid extraction using solutions of binary metal ions (Hg^{2+}/Fe^{3+}, Hg^{2+}/Co^{2+}, Hg^{2+}/Cd^{2+}, Hg^{2+}/Pb^{2+} and Hg^{2+}/Zn^{2+}) resulting in 85.7–90.5% of Hg^{2+} ion being adsorbed by **AR-SiO$_2$** (Fig. 5). In contrast, other metal ions such as Zn^{2+}, Cd^{2+}, Pb^{2+} and Zn^{2+} were extracted into the solid phase at percentages of only 2.5–5.2% in the competition system. These results suggest that **AR-SiO$_2$** is a useful adsorbent for the selective separation of Hg^{2+} over a range of transition and heavy metal ions.

Coloration of TiO_2 films with metal ions

We now address the metal cation sensing ability of **AR-TiO$_2$** films. For the cation sensing experiments, the **AR-TiO$_2$** films were dipped into cation solutions of interest, then dried in air, with any color change determined by "naked-eye" inspection and by measurement of solid UV-vis absorption spectra. In all cases, changes in film color were found to be complete within 1–2 s of immersion, with the resulting coloration being stable for in excess of one day, both for films immersed continuously in the cation solution and for films dried in air. Typical data are shown in Fig. 6, showing a photographic image of the films after immersion in 1.0 mM solutions of chloride salts of the seven cations (Co^{2+}, Cd^{2+}, Pb^{2+}, Zn^{2+}, Fe^{3+}, Cu^{2+} and Hg^{2+}). The yellow color of the **AR-TiO$_2$** film changed to a deep red color when the film was dipped in Hg^{2+} solution. On the other hand, no significant color changes were observed with the other metal ions. These results indicate that the **AR-TiO$_2$** film selectively detected only the Hg^{2+} ion. Since the preparation of the **AR-TiO$_2$** films prepared in this work is much simpler than the sol–gel grafting method, we propose that this **AR-TiO$_2$** film is highly useful as a chemosensor to detect Hg^{2+} ions.

We also observed the solid UV-vis spectra of the **AR-TiO$_2$** films after dipping into the various cation solutions. Fig. 7 shows the corresponding absorption spectra for selected films. It is apparent that the film coloration is only sensitive to the Hg^{2+} ion. Hg^{2+} exposure resulted in a deep red coloration of the film caused by a shift of the absorption maximum from 310 to 492 nm. This bathochromic shift is similar to that observed for **AR-SiO$_2$**. On the other hand, no significant changes in the UV-vis spectra were observed for any other cations tested (including Co^{2+}, Cd^{2+}, Pb^{2+}, Zn^{2+}, Fe^{3+} and Cu^{2+}) for concentrations up to 1.0 mM. Furthermore, the bathochromic shift observed with the Hg^{2+} ion was insensitive to the presence of other cations in the solution, indicating that other metal cations do not interfere with the ability of **AR-TiO$_2$** to detect Hg^{2+}.

The color change observed following the dipping of **AR-TiO$_2$** into Hg^{2+} solution (1.0 μM) was found to be fully reversible when **AR-TiO$_2$** was rinsed thoroughly with EDTA (10.0 μM). Reusability was evaluated by repeated dipping/rinsing cycles, with the **AR-TiO$_2$** absorption spectrum being recorded after each step. Typical data are shown in Fig. 8. The data show that **AR-TiO$_2$** exhibits excellent reusability, as almost no loss in **AR-TiO$_2$** sensitivity was observed after eight repeated dipping/rinsing cycles. In addition, the **AR-TiO$_2$** film before and after dipping of Hg^{2+} ion solution showed transparency with a deep red color (Fig. S14, ESI).†

To develop the **AR-TiO$_2$** as a general Hg^{2+} ion sensor which is independent of any anions present, we also added the anions as I^-, Br^-, NO_3^- and ClO_4^-. With the anion addition, the color of

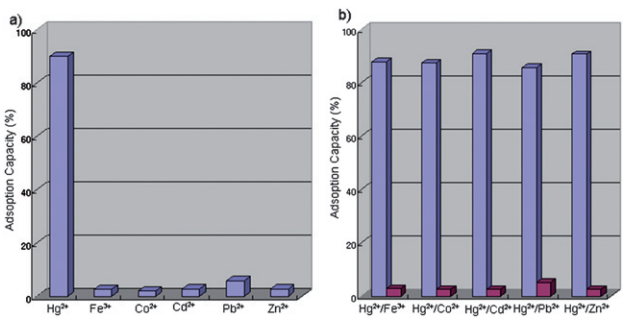

Fig. 5 Adsorption capacities of **AR-SiO$_2$** for (a) single and (b) binary metal ions in H_2O.

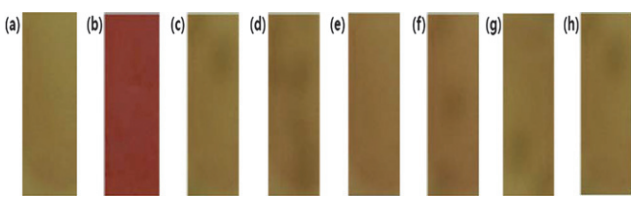

Fig. 6 Color changes observed after the **AR-TiO$_2$** films were dipped in 1.0 mM aqueous solutions of the analytes: (a) the absence and the presence of (b) $HgCl_2$, (c) $CoCl_2$, (d) $CdCl_2$, (e) $PbCl_2$, (f) $ZnCl_2$, (g) $FeCl_3$ and (h) $CuCl_2$.

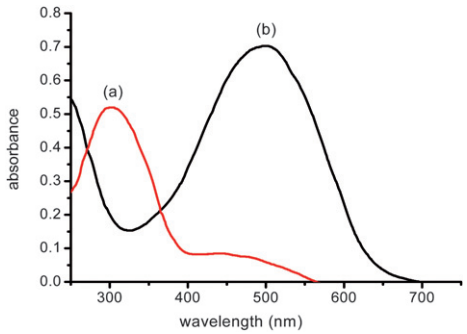

Fig. 7 (A) Solid UV-vis spectra of **AR-TiO$_2$** films in the (a) absence and (b) the presence of $HgCl_2$ (1.5 μM) aqueous solution.

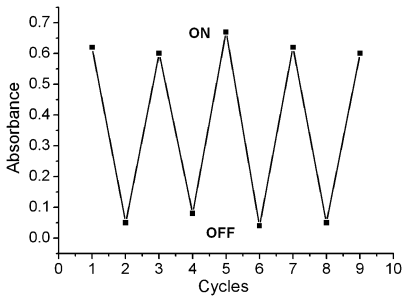

Fig. 8 Plot for the absorbance of **AR-SiO$_2$** by alternated dipping in 1.0 μM aqueous solution of Hg^{2+} ion ("ON") and 10.0 μM EDTA ("OFF"). The cyclic index is the number of alternating dipping/rinsing cycles, with the vertical axis showing the absorbance for the **AR-SiO$_2$** at 492 nm.

the **AR-TiO$_2$** in $HgCl_2$ solution still changed from yellow to deep red. This finding indicates that **AR-TiO$_2$** can be employed for the detection of Hg^{2+} independently of other anion(s) present.

Fig. S15 (ESI)† shows standard calibration data (Abs. *vs.* [Hg^{2+}]) for **AR-TiO$_2$**. A linear response is observed (between 28 nM and 1.0 μM) with a sensitivity of ~28 nM. This sensitivity is much higher than those previously reported for spectrophotometric sensors anchored to mesoporous aluminosilicates.[24] Furthermore, the sensitivity of the **AR-TiO$_2$** film for Hg^{2+} was much higher than that of **AR-SiO$_2$**, because **AR-TiO$_2$** films are transparent and/or have higher immobilization of receptor onto TiO_2 nanoparticles. These findings demonstrate that **AR-TiO$_2$** has strong potential as a portable chemosensor for Hg^{2+} ions.

AR-TiO$_2$ film function as a pH buffer

We consider next the buffer action of the **AR-TiO$_2$** film. The **AR-TiO$_2$** film was immersed in aqueous solutions with pH values ranging between 1.0 and 11.0. Control experiments were conducted using 1.0 mM of Hg^{2+} solution controlling the pH range. The resulting film coloration is shown in Fig. 9. The absorbances of **AR-TiO$_2$** in the presence of Hg^{2+} ion were almost constant, with pH values ranging between 4 and 11. The absorbances of **AR-TiO$_2$** are independent between pH 4 and 11. We conclude that **AR-TiO$_2$** can reliably detect the Hg^{2+} ion over the wide pH range of pH 4–11.

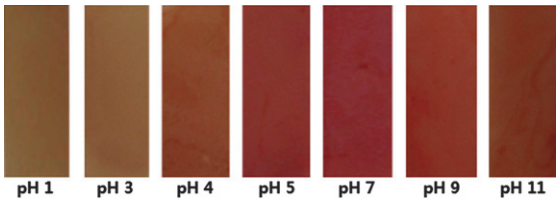

Fig. 9 Color changes observed after **AR-TiO$_2$** films were dipped in Hg^{2+} aqueous solution (1.0 mM) at different pH values.

Conclusions

We have fabricated **AR-SiO$_2$** and **AR-TiO$_2$** using a functional azobenzene-coupled acyclic receptor. The **AR-SiO$_2$** recognized and separated Hg^{2+} with a high degree of selectivity among heavy metal ions in aqueous solution. Beyond its immediate applications in environmental cleanup, **AR-SiO$_2$** provides a unique opportunity to introduce molecular binding sites and to rationally design the surface properties of inorganic nanomaterials. Furthermore, **AR-TiO$_2$** films with 4 μm thickness on glass substrates were prepared as portable chemosensors for Hg^{2+} ion in aqueous solution. The **AR-TiO$_2$** films show excellent sensitivity and selectivity for Hg^{2+} ion. The **AR-TiO$_2$** film detected Hg^{2+} in pH = 7.4 with a sensitivity of 28 nM. The Hg^{2+} detection ability was unaffected by the presence of other cations or anions. The results imply that the **AR-TiO$_2$** film has strong potential as a portable colorimetric sensor for detection of Hg^{2+} in the environmental field. We believe the combination of well-defined inorganic nanomaterials and functionalized organic receptors can play a pivotal role in the development of a new generation of hierarchical structures and functionalized composites.

Acknowledgements

This work was supported by Korea Science and Engineering Foundation Grant (2009-0074100, 2008-2001014), and World Class University (WCU) Program supported from Ministry of Education, Science and Technology (R32-2008-000-20003-0), and Environmental-Fusion Project (191-091-004) supported from Ministry of Environment.

References

1 G. K. Walkup and B. Imperiali, *J. Am. Chem. Soc.*, 1996, **118**, 3053.
2 A. Miyawaki, J. Llopis, R. Helm, J. M. McCaffery, J. A. Adams, M. Ikura and R. Y. Tsien, *Nature*, 1997, **388**, 882.
3 M. M. Henary and C. J. Fahrni, *J. Phys. Chem. A*, 2002, **106**, 5210.
4 J. Homola, S. S. Yee and G. Gauglitz, *Sens. Actuators, B*, 1999, **54**, 3.
5 F. Turner, *Science*, 2000, **290**, 1315.
6 P. Chen and C. He, *J. Am. Chem. Soc.*, 2004, **126**, 728.
7 S. J. Lee, J. –E. Lee, J. Seo, I. Y. Jeong, S. S. Lee and J. H. Jung, *Adv. Funct. Mater.*, 2007, **17**, 3441.
8 S. J. Lee, S. S. Lee, J. Y. Lee and J. H. Jung, *Chem. Mater.*, 2006, **18**, 4713.
9 E. Palomares, R. Vilar, A. Green and J. R. Durrant, *Adv. Funct. Mater.*, 2004, **14**, 111.
10 E. C. Lima, J. L. Brasil and A. H. D. P. Santos, *Anal. Chim. Acta*, 2003, **484**, 233.
11 E. C. Lima, J. L. Brasil and J. C. P. dos Vaghetti, *Talanta*, 2003, **60**, 103.
12 N. G. Becka, R. P. Franks and K. W. Bruland, *Anal. Chim. Acta*, 2002, **455**, 11.
13 E. Palomares, R. Vilar and J. R. Durrant, *Chem. Commun.*, 2004, 362.

14 J. S. Wu, I.-C. Hwang, K. S. Kim and J. S. Kim, *Org. Lett.*, 2007, **9**, 907.
15 M. H. Lee, J. S. Wu, J. W. Lee and J. S. Kim, *Org. Lett.*, 2007, **9**, 2501.
16 E. M. Nolan and S. J. Lippard, *Chem. Rev.*, 2008, **108**, 3443.
17 S. O. Obare, R. E. Hollowell and C. J. Murphy, *Langmuir*, 2002, **18**, 10407.
18 T. Balaji, S. A. El-Safty, H. Matsunaga, T. Hanaoka and F. Mizukami, *Angew. Chem., Int. Ed.*, 2006, **45**, 7202.
19 E. Palomares, M. V. Martínez-Díaz, T. Torres and E. Coronado, *Adv. Funct. Mater.*, 2005, **15**, 803.
20 R. Metivier, I. Leray, B. Lebeau and B. Valeur, *J. Mater. Chem.*, 2005, **15**, 2965.
21 M. Boiocchi, M. Bonizzoni, L. Fabbrizzi, G. Piovani and A. Taglietti, *Angew. Chem., Int. Ed.*, 2004, **43**, 3847.
22 M. H. Lee, S. J. Lee, J. H. Jung and J. S. Kim, *Tetrahedron*, 2007, **63**, 12087.
23 S. J. Lee, J. H. Jung, J. Seo, I. Yoon, K.-M. Park, L. F. Lindoy and S. S. Lee, *Org. Lett.*, 2006, **8**, 1641.
24 A. B. Descalzo, D. Jimenz, J. E. Haskouri, D. Beltran, P. Amoros, M. D. Marcos, R. Martinez-Manez and J. Soto, *Chem. Commun.*, 2002, 562.
25 E. Palomares, R. Vilar, A. Green and J. R. Durrant, *Adv. Funct. Mater.*, 2004, **14**, 111.
26 W. S. Han, H. Y. Lee, S. H. Jung, S. J. Lee and J. H. Jung, *Chem. Soc. Rev.*, 2009, **38**, 1904.
27 H. J. Kim, S. J. Lee, S. Y. Park, J. H. Jung and J. S. Kim, *Adv. Mater.*, 2008, **20**, 3229.
28 H. Y. Lee, D. R. Bae, J. C. Park, H. Song, W. S. Han and J. H. Jung, *Angew. Chem., Int. Ed.*, 2009, **48**, 1239.
29 J. V. Ros-Lis, R. Casasús, M. Comes, C. Coll, M. D. Marcos, R. Martínez-Máñez, F. Sancenón, J. Soto, P. Amorós, J. E. Haskouri, N. Garró and K. Rurack, *Chem.–Eur. J.*, 2008, **14**, 8267.
30 D. Li, A. Wieckowska and I. Willner, *Angew. Chem., Int. Ed.*, 2008, **47**, 1.

